PARAMETRIC FORCING APPROACH FOR SECONDARY MOTIONS FORMATION OVER INHOMOGENEOUS ROUGH SURFACES

A. Stroh[1]*, K. Schäfer*[1]*, B. Frohnapfel*[1] *and P. Forooghi*[2]

[1]*Institute of Fluid Mechanics, Karlsruhe Institute of Technology, Karlsruhe, Germany*
[2]*Department of Engineering, Aarhus University, Aarhus, Denmark*

alexander.stroh@kit.edu

Abstract

A set of direct numerical simulations is used to analyse the application of the so-called parametric forcing approach (PFA), which allows computationally cheaper simulations, instead of high-resolution immersed boundary method (IBM) for modelling of a homogeneous and inhomogeneous rough surface. It is observed that while the PFA delivers excellent agreement for homogeneous case, the agreement between IBM and PFA is rather limited for the inhomogeneous roughness. While secondary motion topology can be successfully reproduced with the PFA approach, the modification of the mean velocity profile and hence integral flow properties cannot be entirely matched between the two approaches. It is shown that the application of homogeneous forcing to an inhomogeneous configuration might lead to deviation of the introduced forcing in the regions where topographical transition occurs so the global drag is altered.

1 Introduction

Formation of secondary motions of Prandtl's second kind is observed in turbulent boundary layer flows subjected to a spanwise inhomogeneity of the near-wall flow field [2]. The spanwise inhomogeneity alters local turbulent properties of the flow and introduces distinct gradients into the Reynolds stress distribution, which eventually manifests in the presence of large-scale vortex pairs occupying the entire boundary layer thickness and significantly modifies the mean velocity profile [7]. The presence of secondary flow translates into an enhancement of momentum and heat transfer, which is of great interest from atmospherical, geological and technical point of view. However, in spite of the seemingly straightforward formation mechanism behind this phenomenon, its physical interpretation, reliable prediction and impact on the local distributions of friction and heat transfer on the wall surface are still being discussed in literature.

Due to the vast parameter space and flow complexity it is still impossible to establish a direct link between the surface topography and corresponding secondary flow. Besides that, investigations of flow over surface structuring pose further difficulties: while on the experimental side it is challenging to capture the flow dynamics associated to secondary motion formation in the vicinity of structuring, the direct numerical simulations (DNS) are often limited by the requirements of fine resolution meshes and hence are extremely expensive from the computational point of view. In order to overcome these limitations and avoid high-resolution meshes a simplified roughness modelling can be utilized: a rough surface can be represented as a wall boundary condition [9] or as an additional forcing term in the near-wall region [1].

(a)

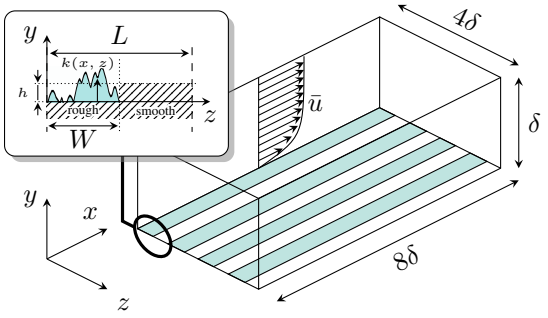

Figure 1: Schematic of the numerical domain with roughness stripes at the walls.

In the present contribution we perform DNS with a simplified parametric forcing approach (PFA) proposed by Busse & Sandham [3] and further extended by Forooghi *et al.* [5] for a simulation of inhomogeneous roughness stripes and compare the results to fully-resolved roughness DNS results reported by Stroh *et al.* [8] in respect to global flow properties and secondary motion formation.

2 Methodology

The secondary motion are studied in a DNS of a fully developed turbulent open channel flow driven by constant pressure gradient (CPG). However, since the introduction of various rough surfaces alters the channel cross-sectional area and hence the effective channel half height δ_{eff}, the pressure gradient $P_x = \tau_{\text{eff}}/\delta_{\text{eff}}$ is adjusted to maintain the friction Reynolds number $Re_\tau = u_\tau \delta_{\text{eff}}/\nu = 500$ across all cases. In stream-

*Corresponding authors Email: alexander.stroh@kit.edu

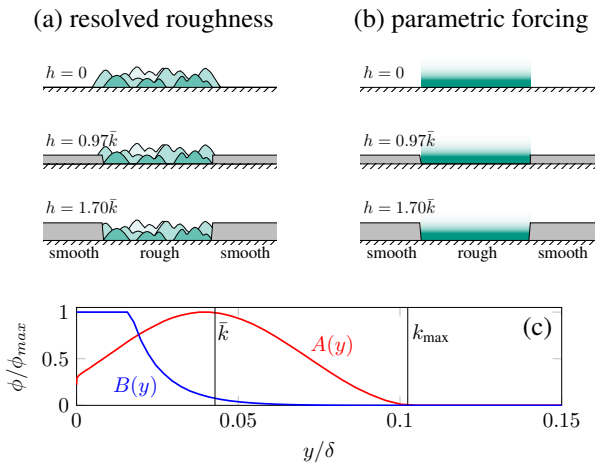

Figure 2: Introduced variation of the smooth wall elevation with resolved (a) and modelled (b) roughness and parametric forcing functions A and B (c).

wise (x) and spanwise direction (z) periodic boundary conditions are used and the wall-normal direction (y) is bounded by no-slip condition at the lower domain ($y = 0$) and symmetry boundary condition at the upper domain ($y = \delta$) as shown in Figure 1(a). The Navier-Stokes equations are integrated by the spectral solver SIMSON [4] with the elevated smooth surfaces represented by the immersed boundary method (IBM) proposed by Goldstein [6].

The width of one alternating smooth and rough wall pattern amounts $L = \delta$, where the roughness width is $W = 0.5\delta$. In Figure 2(a) the three different rough and smooth surface combinations from Stroh *et al.* [8] are presented with the position of the smooth wall at $h = 0$, representing a protruding roughness, at $0.97\bar{k}$, mimicking a roughness which consists of equal contributions of deposition and erosion and at $1.70\bar{k}$, a roughness generated by erosion or corrosion. In Figure 2(b) shows the corresponding configuration, where the parametric forcing is used to represent the rough stripes. For the resolved cases roughness stripes are introduced by the immersed boundary method, while for the cases with modelled roughness stripes the parametric forcing approach by Forooghi *et al.* [5] is utilized. The parametric forcing model augments the Navier-Stokes equations with an additional forcing term active in the area below the plane of the highest roughness peak and represents the average resistance force of the particular roughness topography. The forcing term is $f_i = -A(y)u_i - B(y)u_i\,|u_i|$, where the wall-normal distribution $A(y)$ and $B(y)$ represent viscous and inertial resistance, respectively. The functions $A(y)$ and $B(y)$ as shown in Figure 1(c) are determined for the homogeneously rough case based on the geometrical definition provided in Forooghi *et al.* [5]. Both functions are iteratively tuned via introduction of a constant prefactor for each function, $A(y)$ and

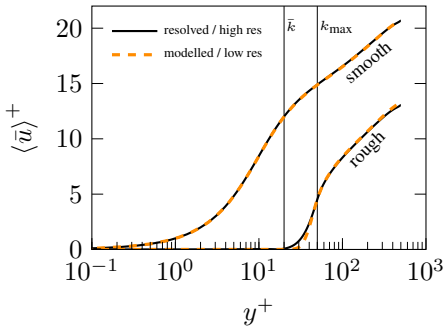

Figure 3: Mean velocity profile of smooth and rough simulations.

Table 1: Integral flow properties for the considered roughness configurations.

case	Re_b	U_b^+	c_f/c_f^s
smooth high res	9051	18.09	1.00
smooth low res	9045	18.09	1.00
$h=0$ resolved	5756	11.52	2.47
$h=0$ modelled	5909	11.82	2.34
$h=0.97k$ resolved	5982	11.96	2.29
$h=0.97\bar{k}$ modelled	6005	12.01	2.27
$h=1.70k$ resolved	6050	12.10	2.24
$h=1.70\bar{k}$ modelled	5961	11.93	2.30
rough resolved	5241	10.47	2.99
rough modelled	5229	10.45	3.00

$B(y)$, until the skin friction coefficient $c_f = 2u_\tau^2/U_b^2$ of the modelled case coincides with the resolved rough case. Botch functions remain constant for all considered simulation with modelled roughness stripes. It has to be noted that the distributions depend only on y and remain homogeneous within the rough stripe area in spanwise and streamwise direction.

The domain size is $(L_x \times L_y \times L_z) = (8\delta \times \delta \times 4\delta)$ with $384 \times 201 \times 384$ grid nodes (referred to as low resolution grid) utilized for the parametric forcing simulations instead of $768 \times 301 \times 384$ grid nodes (referred to as high resolution grid) originally utilized in the reference simulations by Stroh *et al.* [8]. The simulations carried out with parametric forcing on the low resolution grid are also compared with their counterpart on high resolution grid in order to check the resolution dependency. It is confirmed that the deviation between high resolution and low resolution simulations does not exceed 1% for the intergral flow properties like c_f or U_b.

3 Results

Mean Flow Properties

Figure 3 shows the smooth reference simulation at two grid resolutions and the homogeneously rough simulation in resolved and modelled case. The plot confirms the independence of the achieved solution on the resolution and highlights the satisfactory choice of the forcing distribution functions A and B, which

enables a very good agreement for the mean velocity profiles in the resolved and modelled rough simulations. Table 1 shows the global flow properties for these cases. A negligible deviation (max 0.3%) between the resolved and the modelled cases in the resultant Re_b, c_f and U_b^+ is observed for the entire-surface rough simulations. The deviation for striped cases varies from $1-3\%$ for Re_b, U_b^+ and $1-6\%$ for the ratio c_f/c_f^s – the highest deviation is observed for $h=0$. The modelled roughness simulations consistently overpredict the bulk mean velocity, U_b, and hence underestimate the skin friction coefficient for $h<\bar{k}$ in comparison to the resolved ones. In this region, the c_f values are closer to the asymptotic case with extremely wide stripes at $W=0.5L$, where $c_f=0.5(c_f^s+c_f^r)=2.00c_f^s$ is expected to be fulfilled. The discrepancy can be traced back to the local difference in the turbulent and dispersive stress distributions (not shown here).

Secondary Motion

Figure 4 presents the comparison of the secondary motion and mean velocity distribution for the fully resolved and the modelled roughness stripes. It can be observed that the parametric forcing approach can qualitatively reproduce the large-scale secondary motion and its rotational direction, hence capturing the switch in the sense of rotation, which occurs between $h=0$ and $h=1.70\bar{k}$. The modelled rough stripes also show the trends of mean velocity deformation with upward bulging at $h=0$. The strong downward bulging observed at $h=1.70\bar{k}$ for the resolved case, however, is not captured in the modelled simulation - the bulging can be barely observed for this simulation (Figure 4 (c) vs. (f)). It has to be noted that the case at $h=0.97\bar{k}$ shows the largest deviation in the secondary motion topology compared to its resolved counterpart. This case, however, experiences the weakest secondary motion due to the same mean roughness height on smooth and rough area and hence expected to be very sensitive to the roughness forcing distribution.

In order to further elucidate the topology transition we carried out additional simulations with the parametric forcing approach at $h=0.50\bar{k}, 1.25\bar{k}, 1.50\bar{k}, 2.00\bar{k}$ and $2.50\bar{k}$. The results of the parameter variation is shown in Figure 5. In this figure we can observe two characteristic topology maps – a more complex topology with three counter-rotating vortex pairs with upward streamwise velocity bulging rather corresponding to the ridge-type roughness ($h=0-0.97\bar{k}$) and a single large-scale vortex pair with downward bulging known to be characteristic for the strip-type surfaces ($h=1.70\bar{k}-2.50\bar{k}$). Two cases in the middle show the transition between those two states ($h=1.25\bar{k}, 1.50\bar{k}$). It can be seen that the case at $h=2.00\bar{k}$ topologically rather corresponds to the resolved case $h=1.70\bar{k}$, which indicates that the parametric forcing approach in induces a slightly different effect on the turbulent flow properties. Based on the comparison one might hypothesize that the parametric forcing approach introduces a slightly higher roughness layer and hence a smooth wall at higher position is needed to obtain similarly strong bulging of the mean velocity profile.

Figure 6 summarizes the resulting skin friction coefficient from the entire set of simulations as a function of smooth wall elevation h. It is observed that the modelled roughness cases in the transitional state, where the weakest secondary motion is formes ($h=1.25\bar{k}, 1.50\bar{k}$) show the lowest skin friction coefficient, while the strip- and ridge-type roughness cases below $h=\bar{k}$ and above $h=1.70\bar{k}$ with rather strong secondary motion show a higher skin friction coefficient. Due to the limited amount of resolved simulations the profile for c_f shows a decreasing trend for h up to $1.70\bar{k}$.

Forcing Comparison

Figure 7 demonstrates the comparison of the streamwise (f_x), wall-normal (f_y) and spanwise (f_z) mean force exerted by the immersed boundary method and the parametric approach for $h=0.97\bar{k}$. For the resolved streamwise component f_x we observe a diffuse forcing region resembling the shape of the roughness elements. It has to be emphasized that the diffuse are extends down to the lower wall. This is linked to the fact that in the IBM case the roughness consists of locally distributed elements, hence the local surface force is also distributed in the wide range within the roughness layer. Interestingly, the wall-normal forcing f_y for IBM shows a distinct negative region around the top of the roughness elements, while the lower part is rather positive. This is related to the fact that the IBM approach enforces the flow to follow the curvature of the introduced geometry, so a deflection towards the wall is imposed on the element peaks, while the positive area represents the windward side of the elements, where a wall-normal deflection away from the wall must be imposed. The spanwise forcing f_z represents the flow deflection around the roughness elements and also resembles the introduced geometrical shape of the roughness. It has to be noted that the negative streamwise forcing is around 5 times stronger than the forcing observed for wall-normal and spanwise direction. For the PFA the force is applied only to streamwise and spanwise velocity component, so f_y is zero. The streamwise force is rather concentrated in the area $y>\bar{k}$, while for $y<\bar{k}$ it barely shows any presence of forcing. Due to the spanwise homogeneity of the PFA we also observe a very homogeneous distribution for f_x within the roughness region. The spanwise component of the force f_z shows two peaks concentrated around the corners, where the transition from the smooth to rough and vice versa occurs. At this point it is obvious, that the two approaches, IBM and PFA, produce different force distribution when the rough region is combined with a smooth wall in the

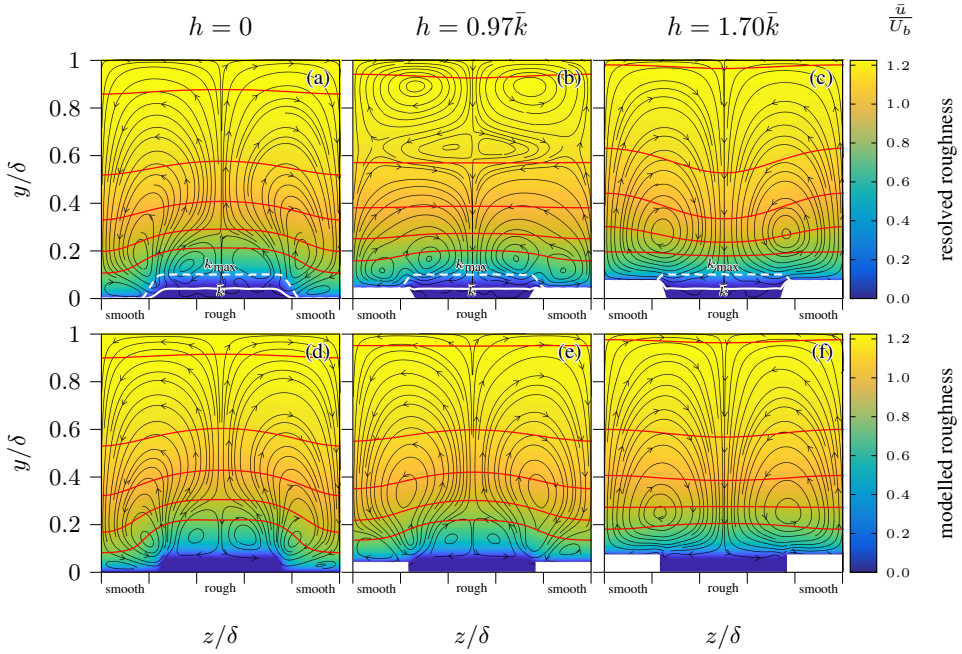

Figure 4: Mean velocity profile at different elevation of the smooth stripes for resolved roughness (a-c) and modelled roughness (d-e). Black lines indicate time-averaged streamlines of secondary motion in y-z-plane, red solid lines mark the isolines of the streamwise mean velocity distribution.

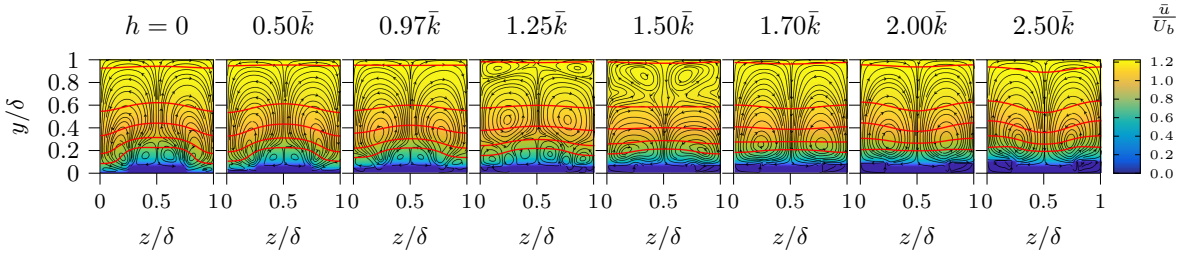

Figure 5: Evolution of secondary flow topology for parametric forcing approach with increasing smooth wall position.

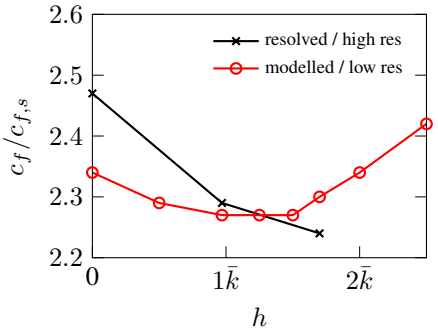

Figure 6: Skin friction coefficient dependency on the smooth wall height h for IBM (resolved) and PFA (modelled) approach.

same configuration.

In Figure 8 we compare the streamwise mean force introduced by IBM and PFA in the corner regions, in the middle of the rough region at $h = 0.97\bar{k}$ and the force for homogeneous rough case. It is observed that for both approaches the striped configurations produces a slightly stronger forcing in the middle of the roughness stripes (dashed vs. solid lines), however, the distribution of the forcing remains similar to their homogeneous counterpart. In the corner regions at $z = 0.26\delta$ the resolved approach introduces almost the same forcing distribution as in the middle of the rough surface at $z = 0.5\delta$, while the parametric forcing induces significantly stronger forcing at the corners (around two times larger magnitude) in comparison to the position in the middle of the rough area. This might indicate that the parametric forcing acts in a different manner in an inhomogeneous configuration and cannot capture the entire flow alteration effects introduced by the resolved roughness.

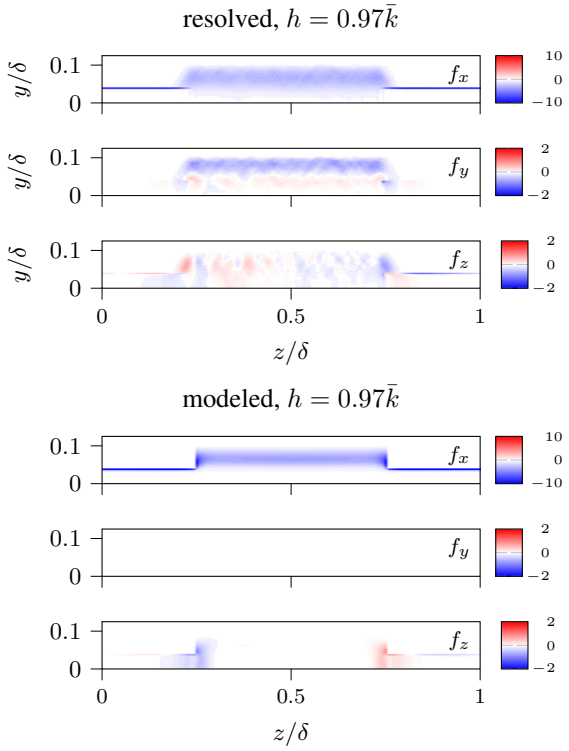

Figure 7: Comparison of the mean force $f_i\bar{k}/u_\tau^2$ exerted by the IBM and PFA approach at $h = 0.97\bar{k}$. Dashed vertical lines mark the position of forcing compared in Fig. 8.

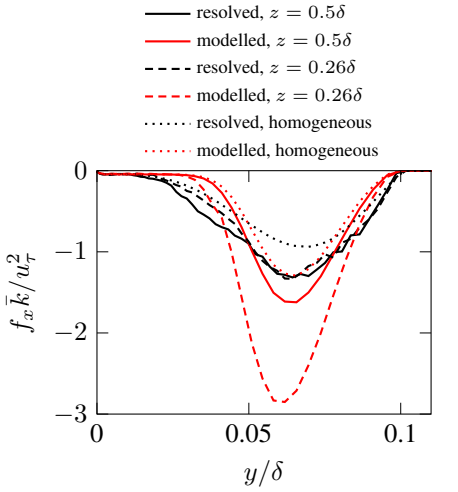

Figure 8: Comparison of the exerted local forcing at $h = 0.97\bar{k}$ in the middle of rough stripe at $z = 0.5\delta$ (solid), close to the corner at the position $z = 0.26\delta$ (dashed) between IBM (resolved) and PFA (modelled) approach. Forcing for the homogeneous roughness is also shown for comparison (dotted).

4 Conclusion & Outlook

A parametric forcing approach is used to model rough surfaces in a DNS of a turbulent open channel flow. It is found that while the model performs well for the homogeneous roughness, an application of the model with the same forcing distribution used for inhomogeneous roughness case can acceptably reproduce the secondary motions topology and magnitude. However, a discrepancy in the resultant bulk mean velocity and skin friction coefficient is observed. The analysis of exerted forcing for IBM and PFA confirms several differences in the forcing distributions, which are specifically present at the corner regions where the topographical transition from smooth to rough surface occurs. Future investigations on PFA will aim at providing a deeper understanding of drag generation mechanism related to the introduced forcing and secondary motion with a long-term goal to provide a forcing correction able to improve the prediction of integral flow properties.

Acknowledgments

Support by the German Research Foundation (DFG) under Collaborative Research Centre TRR150 (project number 237267381) is greatly acknowledged. This work was performed on the HoreKa supercomputer funded by the Ministry of Science, Research and the Arts Baden-Württemberg and by the Federal Ministry of Education and Research.

References

[1] W. Anderson and C. Meneveau. A large-eddy simulation model for boundary-layer flow over surfaces with horizontally resolved but vertically unresolved roughness elements. *Bound.-Layer Meteorol.*, 137(3):397–415, 2010.

[2] P. Bradshaw. Turbulent secondary flows. *Annu. Rev. Fluid Mech.*, 19(1):53–74, 1987.

[3] A. Busse and N. D. Sandham. Parametric forcing approach to rough-wall turbulent channel flow. *J. Fluid Mech.*, 712:169–202, 2012.

[4] M. Chevalier, P. Schlatter, A. Lundbladh, and D. Henningson. Simson: A pseudo-spectral solver for incompressible boundary layer flows. 07 2007. TRITA-MEK, KTH Mechanics, Stockholm, Sweden.

[5] P. Forooghi, B. Frohnapfel, F. Magagnato, and A. Busse. A modified parametric forcing approach for modelling of roughness. *Int. J. Heat Fluid Fl.*, 71:200–209, 2018.

[6] D. Goldstein, R. Handler, and L. Sirovich. Modeling a no-slip flow boundary with an external force field. *J. Comput. Phys.*, 105(2):354–366, 1993.

[7] J. Nikuradse. *Untersuchung über die Geschwindigkeitsverteilung in turbulenten Strömungen*. VDI-Verlag, 1926.

[8] A. Stroh, K. Schäfer, B. Frohnapfel, and P. Forooghi. Rearrangement of secondary flow over spanwise heterogeneous roughness. *J. Fluid Mech.*, 885:R5, 2020.

[9] D. Willingham, W. Anderson, K. T. Christensen, and J. M. Barros. Turbulent boundary layer flow over transverse aerodynamic roughness transitions: Induced mixing and flow characterization. *Phys. Fluids*, 26(2):025111, 2014.